Am J Cancer Res 2022;12(6):2594-2611
www.ajcr.us /ISSN:2156-6976/ajcr0143155

Original Article

Receptor interacting protein 1 knockdown induces cell death in liver cancer by suppressing STAT3/ATR activation in a p53-dependent manner

Seung-Youn Jung[1*], Jeong-In Park[1*], Jae-Hoon Jeong[1], Kyung-Hee Song[1], Jiyeon Ahn[1], Sang-Gu Hwang[1], Jaesung Kim[1], Jong-Kuk Park[1], Dae-Seog Lim[2], Jie-Young Song[1]

[1]*Division of Radiation Biomedical Research, Korea Institute of Radiological & Medical Sciences, Seoul 01812, Republic of Korea;* [2]*Department of Biotechnology, CHA University, Gyeonggi-do 13488, Republic of Korea.* [*]*Equal contributors.*

Received March 7, 2022; Accepted May 2, 2022; Epub June 15, 2022; Published June 30, 2022

Abstract: The survival and death of eukaryotic cells are tightly controlled by a variety of proteins in response to the cellular environment. Receptor-interacting serine/threonine-protein kinase 1 (RIPK1) is a receptor-interacting Ser/Thr kinase that has recently been reported as an important regulator of cell survival, apoptosis, and necroptosis; however, its role in liver cancer remains unclear. In this study, we examined the effect of siRNA-mediated RIPK1 knockdown on the survival and death of liver cancer cells. Treatment with siRIPK1 decreased the growth rate of liver cancer cells and increased apoptotic, but not necrotic cell death, which was higher in wild-type p53 (wt-p53) cells than in mutant-type p53 (mt-p53) cells. In addition, RIPK1 knockdown increased p53 expression and G1 phase arrest in wt-p53 cells. Although suppressing p53 did not alter RIPK1 expression, it did attenuate siRIPK1-induced cell death. Interestingly, RIPK1 knockdown also increased the generation of reactive oxygen species and DNA damage by inhibiting signal transduced and activator of transcription 3 (STAT3) and ATM and RAD3-related (ATR) in wt-p53 cells but not in mt-p53 cells. Moreover, STAT3 or ATR inhibition in p53 mutant cells restored siRIPK1-mediated cell death. Together, the results of this study suggest that RIPK1 suppression induces apoptotic cell death by inhibiting the STAT3/ATR axis in a p53-dependent manner. Furthermore, these findings suggest that RIPK1, alone or in combination, may be a promising target for treating liver cancer.

Keywords: Apoptosis, ATR, liver cancer, p53, RIPK1, STAT3

Introduction

The fate of eukaryotic cells is strictly determined by proteins that regulate cell survival or death in response to different cellular situations. Programmed and unprogrammed cell death, also known as apoptosis and necrosis, respectively, are well defined forms of cell death that have been studied for several decades [1]. However, a type of programmed necrosis, termed necroptosis, was recently identified and shown to be induced by factors such as tumor necrosis factor-alpha (TNF-α), as well as TNF-related apoptosis-inducing ligand, Fas ligand, TNF-related weak inducer of apoptosis, lipopolysaccharide, and dsRNA [2-5].

In many cell types, TNF-α-stimulated TNF receptor type 1 (TNFR1) promotes the formation of an intracellular complex consisting of TNFR1-associated death domain proteins and receptor-interacting serine/threonine-protein kinase 1 (RIPK1), which activates the canonical nuclear factor kappa-light-chain-enhancer of activated B cells (NF-κB) survival pathway. The loss of cellular inhibitors of apoptosis proteins and treatment with a second mitochondria-derived activator of caspases mimetic or cycloheximide (CHX) can reduce anti-apoptotic activity, allowing TNF-α to promote the transition from survival to caspase-8-associated apoptosis [3-6]. However, if caspase activity is blocked by carbobenzoxy-valyl-alanyl-aspartyl-[O-methyl]-fluoromethyl ketone (z-VAD-fmk) or viral proteins such as B13R/Spi2 (vaccinia virus), vICA (cytomegalovirus), E3 (adenovirus), E6 (human papillomavirus 16), and p35 (baculovirus), cells undergo necroptosis through RIPK1 and RIPK3 complex formation and mixed lineage kinase

domain-like pseudokinase (MLKL) activation [7-9]. Furthermore, *in vivo* experiments have revealed that RIPK1-deficient mice die shortly after birth due to systemic inflammation, indicating that RIPK1 is a major regulator of cell survival, apoptosis, and necroptosis [3, 4].

Liver cells are often exposed to an inflammatory environment as they play important roles in the detoxification of harmful foods or substances [10]. Indeed, hepatitis B virus (HBV), hepatitis C virus (HCV) infection, and alcohol are major inducers of inflammation and fibrosis that can result in the carcinogenesis of hepatocellular carcinoma (HCC) [11, 12]. Since inflammatory cytokines can also induce RIPK1 activation and necroptosis is associated with the pathology of acute hepatitis, nonalcoholic fatty liver disease, and alcoholic liver disease [4, 7], RIPK1 is considered an attractive target for modulating homeostasis and carcinogenesis in the liver. Although previous studies have demonstrated that RIPK1 is a crucial component of TNF-signaling cascades that protect against infection, inflammation, cellular differentiation, and DNA damage, its specific roles in the absence of exogenous stimuli have not yet been elucidated in liver cancer.

In this study, we aimed to investigate the roles and mechanisms of RIPK1 in liver cancer cells. Notably, RIPK1 knockdown decreased the viability of liver cancer cells and induced apoptosis by inhibiting STAT3-ATR signaling in a p53-dependent manner. Together, these findings suggest the existence of a complex regulatory network between RIPK1, p53, and STAT3, and indicate that different therapeutic approaches should be considered for patients with liver cancer depending on their p53 status.

Materials and methods

Materials

Primary antibodies against cleaved caspase-3, PARP, and p-ATR (S428) were obtained from Cell Signaling Technology (Danvers, MA, USA); γH2AX and p53 from Santa Cruz Biotechnology (Santa Cruz, CA, USA); RIPK1 from BD Biosciences (Palo Alto, CA, USA); and GAPDH from AbFrontier (Seoul, Korea). Horseradish peroxidase (HRP)-conjugated secondary antibodies were purchased from Thermo Fisher Scientific (Waltham, MA, USA).

Cell culture and transfection

HepG2, SK-Hep-1, Huh-7, and SNU449 cells were maintained in RPMI 1640 supplemented with 10% fetal bovine serum (Gibco, Grand Island, NY, USA), 100 U/mL penicillin, and 100 μg/mL streptomycin in a humidified 5% CO_2 atmosphere at 37°C. To suppress RIPK1 expression, cells were seeded onto the appropriate dishes or plates at a density of 10,000-20,000 cells/cm^2. After 24 h, the cells were transfected with RIPK1 and p53 targeted siRNAs and non-targeted scramble (SCR) siRNAs using RNAiMax transfection reagent (Thermo Fisher Scientific) according to the manufacturer's instructions, and analysis was performed. The siRNA sequences were as follows: RIPK1, 5'-GAA CCC AGG GAC UCA UGA UUU-3' (forward) and 5'-AUG AGU CCC UGG GUU CUU-3' (reverse); p53, 5'-UCA GAC CUA UGG AAA CUA CUU UU-3' (forward) and 5'-AAG UAG UUU CCA UAG GUC UGA UU-3' (reverse); STAT3, 5'-GCA CAA UCU ACG AAG AAU CAA UU-3' (forward) and 5'-UUG AUU CUU CGU AGA UUG UGC UU-3' (reverse); ATR, 5'-GAU GAA CAC AUG GGA UAU UUA UU-3' (forward) and 5'-UAA AUA UCC CAU GUG UUC AUC UU-3' (reverse); scramble, 5'-CCU CGU GCC GUU CCA UCA GGU AGU U-3' (forward) and 5'-CUA CCU GAU GGA ACG GCA CGA GGU U-3' (reverse).

3-[4,5-Dimethylthiazol-2-yl]-2,5-diphenyltetrazolium bromide MTT assay

Cell viability was assessed using MTT assays (Sigma-Aldrich; St. Louis, MO, USA). Briefly, each cell line was plated onto 24-well plates (SPL; Gyeonggi, Korea) and transfected with the indicated siRNAs after 24 h. MTT was added directly to each well at a final concentration of 0.5 mg/mL and the medium was removed after 4 h. Intracellular formazan crystals were dissolved in dimethyl sulfoxide and the absorbance of the formazan solution was measured using a Multiskan EX microplate reader (Thermo LabSystems; Waltham, MA, USA) equipped with a 540-nm filter. Each sample was assayed in triplicate, and the experiments were repeated three times.

Western blot analysis

Cells were lysed with RIPA buffer (50 mM Tris-HCl, pH 7.4, 1% NP-40, 150 mM NaCl, and 1 mM EDTA) supplemented with protease inhibi-

tors (1 mM phenylmethylsulfonyl fluoride, 1 μg/mL aprotinin, and 1 μg/mL leupeptin) and phosphatase inhibitors (1 mM Na_3VO_4 and 1 mM NaF). Proteins in the whole-cell lysates were separated on 8-15% SDS-polyacrylamide gels and transferred to nitrocellulose membranes (Bio-Rad, Hercules, CA, USA). The membranes were blocked for 1 h with 5% skim milk in Tris-buffered saline containing 0.1% Tween-20 and then probed with primary antibodies overnight at 4°C. After washing three times, the membranes were incubated with HRP-conjugated secondary antibodies and immunoreactive bands were detected using enhanced chemiluminescence reagents according to the manufacturer's recommendations (GE Healthcare; Little Chalfont, UK). Experiments were repeated at least three times.

Annexin V/Propidium iodide (PI) staining

Apoptotic and necrotic cells were evaluated using an annexin V-APC/PI detection kit (BD Biosciences, San Diego, CA, USA) according to the manufacturer's instructions. Briefly, dead cells in the culture media and attached cells were collected, washed twice with phosphate buffered saline (PBS), and incubated with annexin V-APC and PI for 15 min. Stained cells were measured using a FACScaliber (BD Biosciences) or Cube6 (Partec, Münster, Germany) flow cytometer and analyzed using FlowJo software (v. 10, Tree Star; Ashland, OR, USA).

Cell cycle analysis

Cells were transfected with SCR or RIPK1-targeted siRNAs for 72 h, fixed in 70% cold ethanol overnight, and treated with RNase for 20 min. After 50 μg/mL PI was added, the cells were analyzed using a FACS Calibur instrument (BD Biosciences).

Detection of intracellular reactive oxygen species (ROS)

Cells were transfected with the indicated siRNAs for 72 h, treated with 10 mM CM-H_2DCFDA for 30 min, and then harvested following detachment with trypsin. After the cells had been washed and resuspended in PBS, intracellular ROS levels were detected using a flow cytometer (CyFlow Cube 6) at excitation/emission wavelengths of 488/525 nm.

Bioinformatics analysis

To determine the clinical significance of RIPK1 expression, we analyzed The Cancer Genome Atlas (TCGA) data using the GEPIA2 database. The effects of RIPK1 mRNA and protein expression on overall survival (OS) in liver cancer was analyzed using the Kaplan-Meier Plotter (https://kmplot.com/analysis/). Patients were divided into high and low expression groups using the median expression value. The results from the dataset with the lowest *p*-value for each analysis were presented.

Statistical analysis

Statistical analyses were performed using GraphPad Prism v. 9.0 (GraphPad, La Jolla, CA, USA). All data were expressed as the mean ± standard deviation (SD). Significant differences between groups were determined using analysis of variance (ANOVA) with Tukey's post-hoc test. Data were considered statistically significant at $*P < 0.05$, $**P < 0.01$, and $***P < 0.001$.

Results

RIPK1 suppression reduces the viability of human liver cancer cells

The liver is constantly exposed to noxious stressors and inflammatory stimuli, and RIPK1 is known to regulate cell death and survival [3, 4]; therefore, we investigated basal RIPK1 expression levels in several different human liver cancer cell lines using western blot analysis (**Figure 1A**). Although RIPK1 was expressed in all the cell lines used in this study, RIPK1 expression was higher in SK-Hep-1 and Huh-7 cells than in HepG2, SNU 449, and SNU878 cells, while Chang liver cells also showed considerable RIPK1 expression. To investigate the effect of RIPK1 on cell viability, the cells were transfected with siRNAs that effectively reduced RIPK1 expression (**Figure 1B**) and significantly decreased cell viability (**Figure 1C**). Silencing RIPK1 in HepG2 and SK-Hep-1 cells induced severe cytotoxicity and resulted in numerous floating cells (**Figure 1D**). Thus, these results indicate that RIPK1 expression levels vary in HCC cells and RIPK1 knockdown decreases cell viability to different extents depending on the cell type.

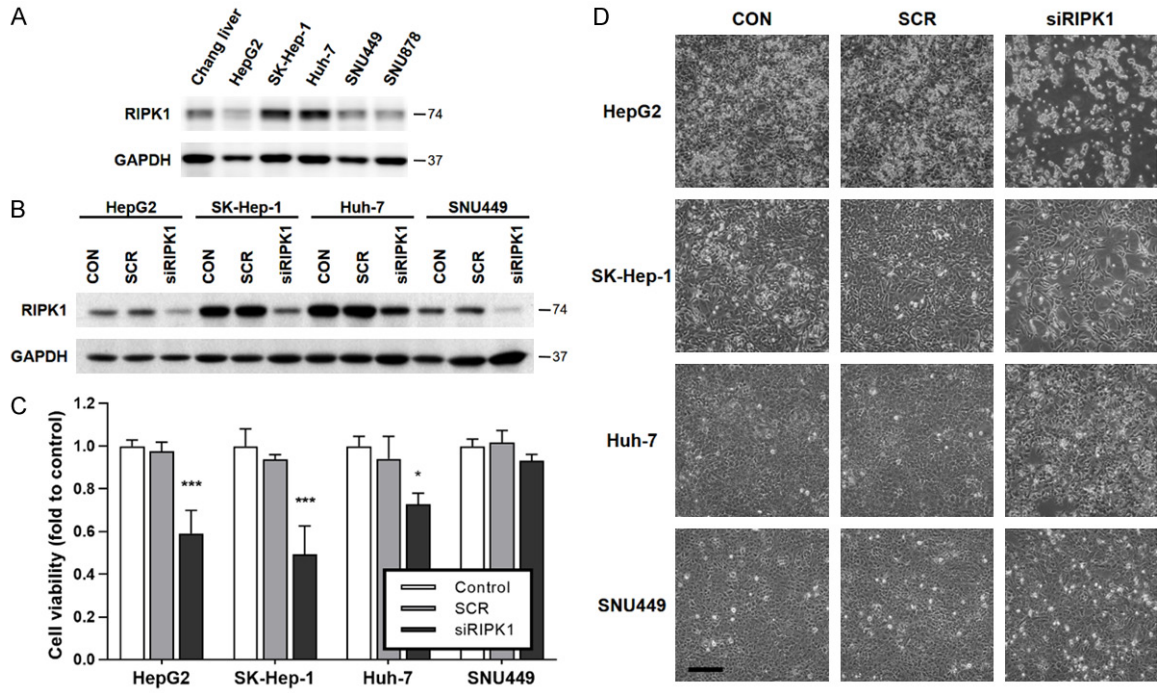

Figure 1. RIPK1 suppression decreases the viability of liver cancer cells. A. Basal RIPK1 expression in several liver cancer cell lines, as examined by western blot analysis using the indicated antibodies. B. RIPK1 expression in the indicated cell lines transfected with non-targeted scrambled siRNA (SCR) or RIPK1-targeted siRNAs for 72 h, as examined by western blot analysis. C. Viability of the indicated cell lines transfected with SCR or RIPK1-targeted siRNAs for 72 h, as examined using MTT assays. D. Morphological changes and viability of the indicated cell lines transfected with SCR or RIPK1-targeted siRNAs for 72 h. The cells were imaged under a microscope at 100× magnification. Scale bar 250 μm.

RIPK1 suppression induces apoptotic cell death

Since RIPK1 knockdown reduced cell viability, we examined whether siRIPK1 treatment also affected apoptotic cell death using annexin V/PI staining (**Figure 2A**, **2B**). The percentage of apoptotic SK-Hep1 and HepG2 cells increased significantly following siRIPK1 treatment, whereas there was little change in the proportion of Huh-7 and SNU-449 cells. In addition, RIPK1 knockdown induced caspase-3 and poly (ADP-ribose) polymerase (PARP) cleavage in all four cell lines to different degrees, confirming that apoptosis had occurred (**Figure 2C**).

The following experiments were performed on only two cell lines wherein apoptosis was markedly increased by siRIPK1. Pretreating HepG2 and SK-Hep1 cells with the apoptosis inhibitor, z-VAD-fmk, significantly reduced apoptosis induction by siRIPK1, as indicated by the reduced number of annexin V-positive apoptotic cells (**Figure 2D**, **2E**). Consistently, immunoblot assays showed that z-VAD-fmk attenuated PARP-1 cleavage induced by RIPK1 suppression (**Figure 2F**). Together, these data suggest that RIPK1 knockdown decreases HepG2 and SK-Hep-1 cell viability by inducing apoptosis.

p53 plays a role in siRIPK1-induced apoptosis

Since HepG2 and SK-Hep-1 cells have been reported to express wt-p53, whereas Huh-7 (Y220C) and SNU449 (A161T) cells express mt-p53 (http://p53.free.fr/), we measured p53 expression following RIPK1 knockdown. As shown in **Figure 3A**, siRIPK1 increased p53 expression in cells with wt-p53 but not mt-p53, whereas the expression of MDM2, a negative regulator of p53, did not change in any of the cell lines. p53 also plays a key regulatory role in the cell cycle and is involved in G1 and G2/M arrest. Notably, RIPK1 knockdown induced G1 arrest in HepG2 cells and increased the apoptotic sub-G1 population of SK-Hep-1 cells while significantly reducing the S/G2M

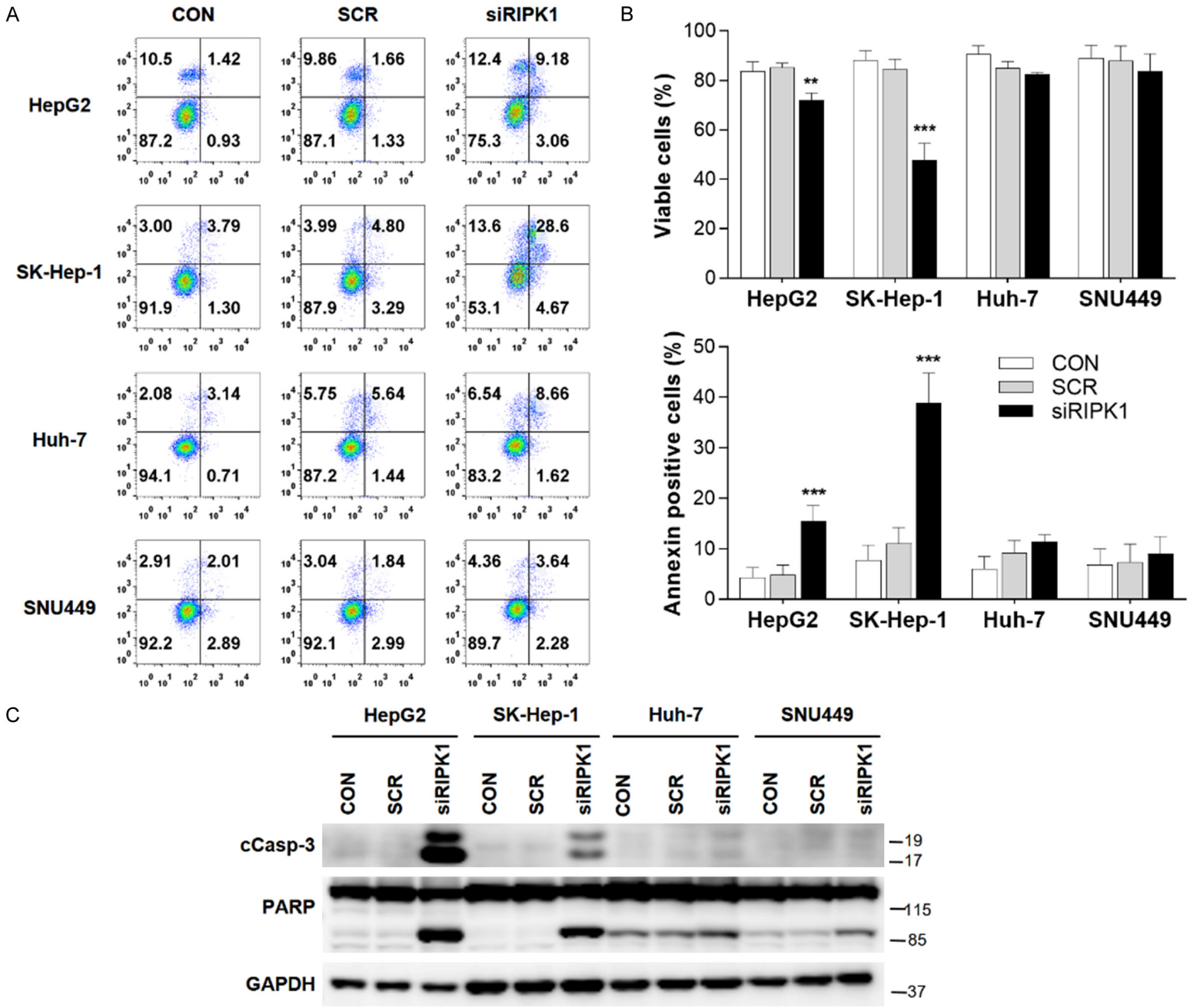
A
CON
SCR
siRIPK1
HepG2
10.5
1.42
87.2
0.93
9.86
1.66
87.1
1.33
12.4
9.18
75.3
3.06
SK-Hep-1
3.00
3.79
91.9
1.30
3.99
4.80
87.9
3.29
13.6
28.6
53.1
4.67
Huh-7
2.08
3.14
94.1
0.71
5.75
5.64
87.2
1.44
6.54
8.66
83.2
1.62
SNU449
2.91
2.01
92.2
2.89
3.04
1.84
92.1
2.99
4.36
3.64
89.7
2.28
B
Viable cells (%)
100
80
60
40
20
0
**
***
HepG2
SK-Hep-1
Huh-7
SNU449
Annexin positive cells (%)
50
40
30
20
10
0
***
***
CON
SCR
siRIPK1
HepG2
SK-Hep-1
Huh-7
SNU449
C
HepG2
SK-Hep-1
Huh-7
SNU449
CON
SCR
siRIPK1
cCasp-3
PARP
GAPDH
19
17
115
85
37

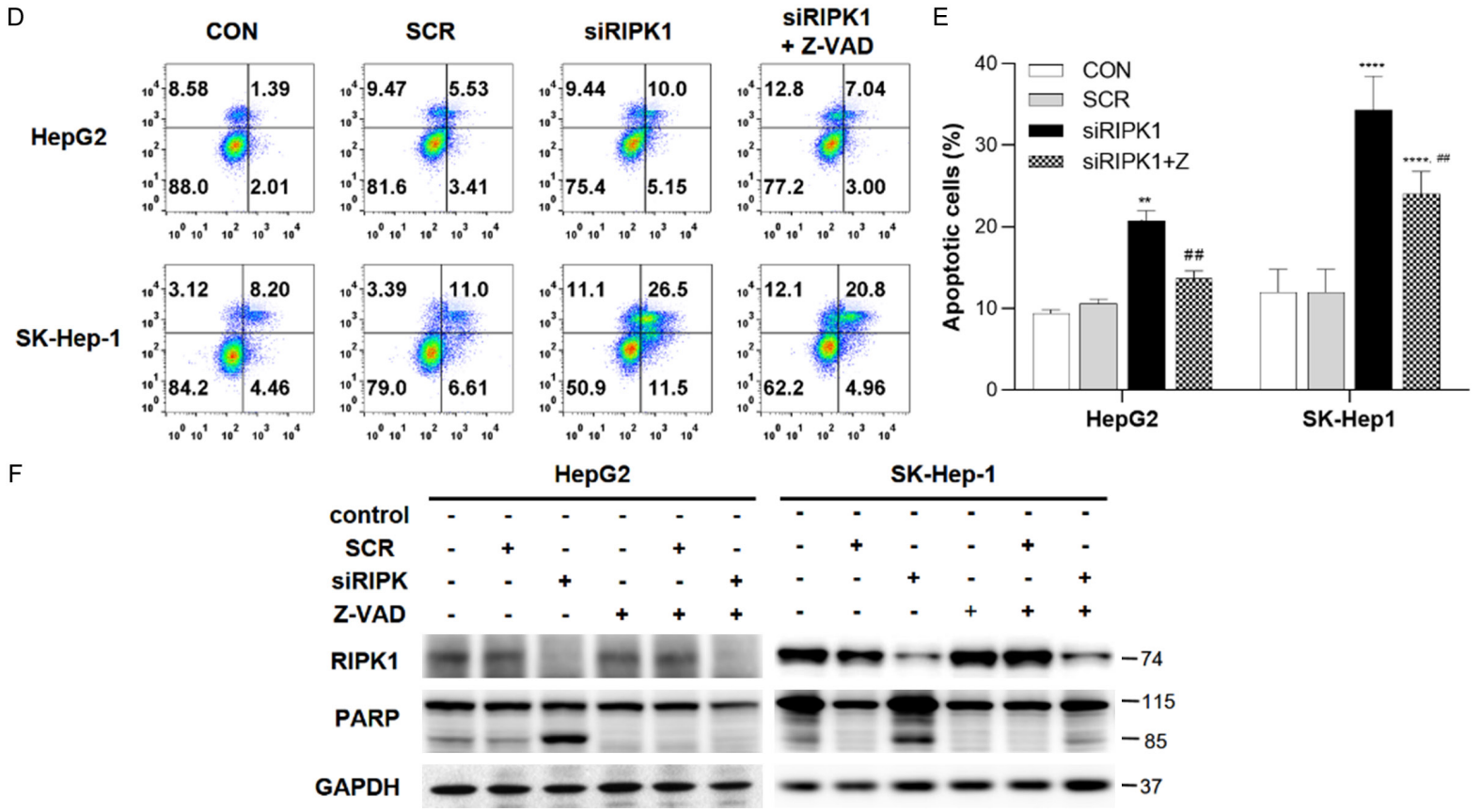

Figure 2. RIPK1 suppression induces apoptosis. A. Annexin V-APC and PI staining in the indicated cell lines transfected with siRNAs for 72 h, as analyzed using FlowJo software. B. Surviving cell population (upper) and Annexin V-positive cell population (lower) in the Annexin V/PI staining. Data represent the percentage ± SD; $^{**}P < 0.01$, $^{***}P < 0.001$ vs. control. C. Cleaved caspase-3 and PARP expression in HCC transfected with siRNAs for 72 h, as examined by western blot analysis using the indicated antibodies. D. Annexin V-APC and PI staining in HepG2 and SK-Hep-1 cells transfected with siRNAs and treated with z-VAD-fmk (20 μM) for 72 h, as analyzed using FlowJo software. E. Annexin V-positive cell populations in the Annexin V/PI staining. Data represent the percentage ± SD; $^{**}P < 0.01$, $^{****}P < 0.0001$ vs. control, $^{\#\#}P < 0.01$ vs. siRIPK1. F. Western blot analysis of HepG2 and SK-Hep-1 cells transfected with siRNAs and treated with z-VAD-fmk.

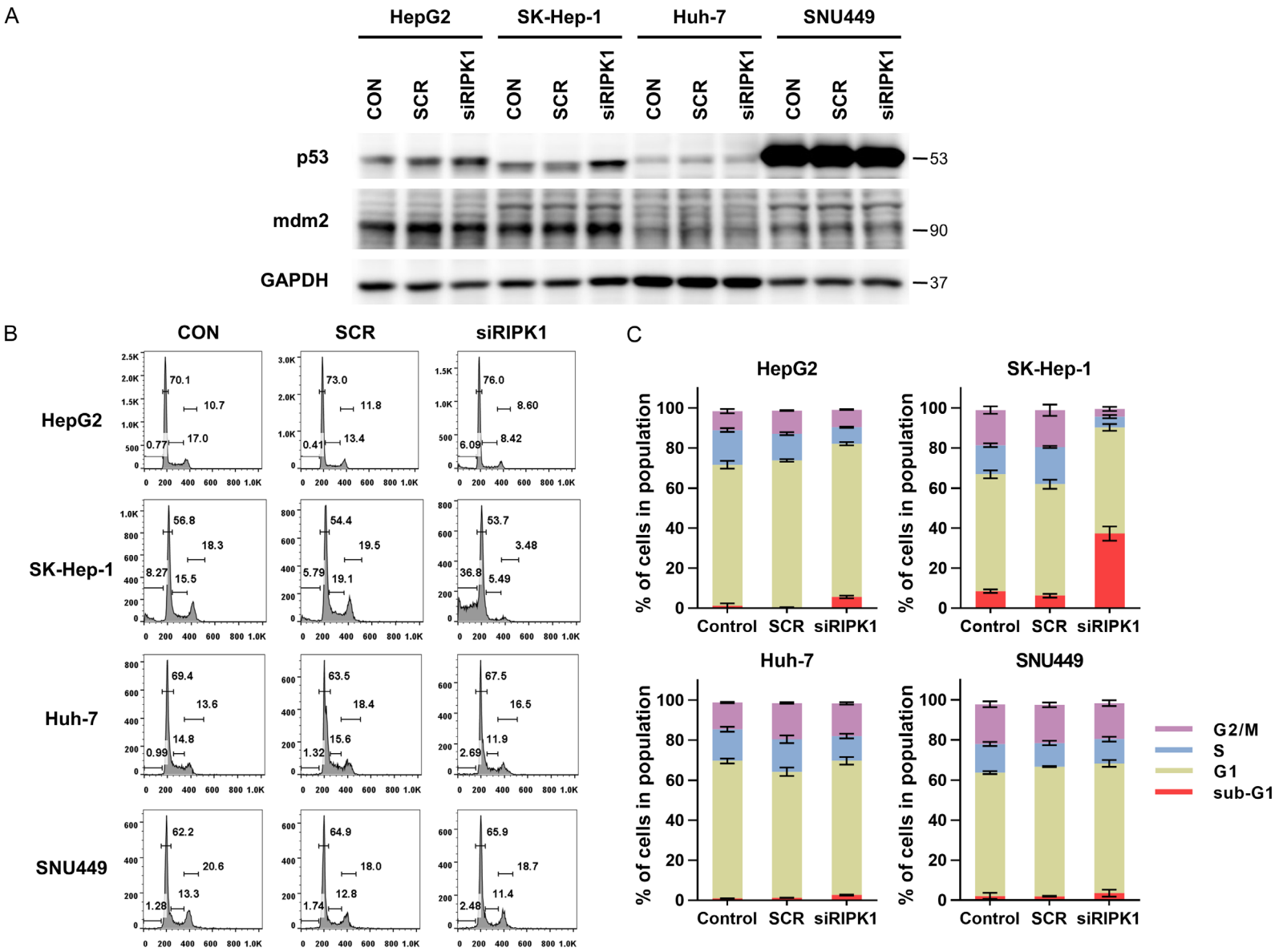
A
HepG2
SK-Hep-1
Huh-7
SNU449
CON
SCR
siRIPK1
p53
mdm2
GAPDH
53
90
37
B
CON
SCR
siRIPK1
HepG2
SK-Hep-1
Huh-7
SNU449
70.1
10.7
0.77
17.0
73.0
11.8
0.41
13.4
76.0
8.60
6.09
8.42
56.8
18.3
8.27
15.5
54.4
19.5
5.79
19.1
53.7
3.48
36.8
5.49
69.4
13.6
0.99
14.8
63.5
18.4
1.32
15.6
67.5
16.5
2.69
11.9
62.2
20.6
1.28
13.3
64.9
18.0
1.74
12.8
65.9
18.7
2.48
11.4
C
HepG2
SK-Hep-1
Huh-7
SNU449
% of cells in population
Control
SCR
siRIPK1
G2/M
S
G1
sub-G1

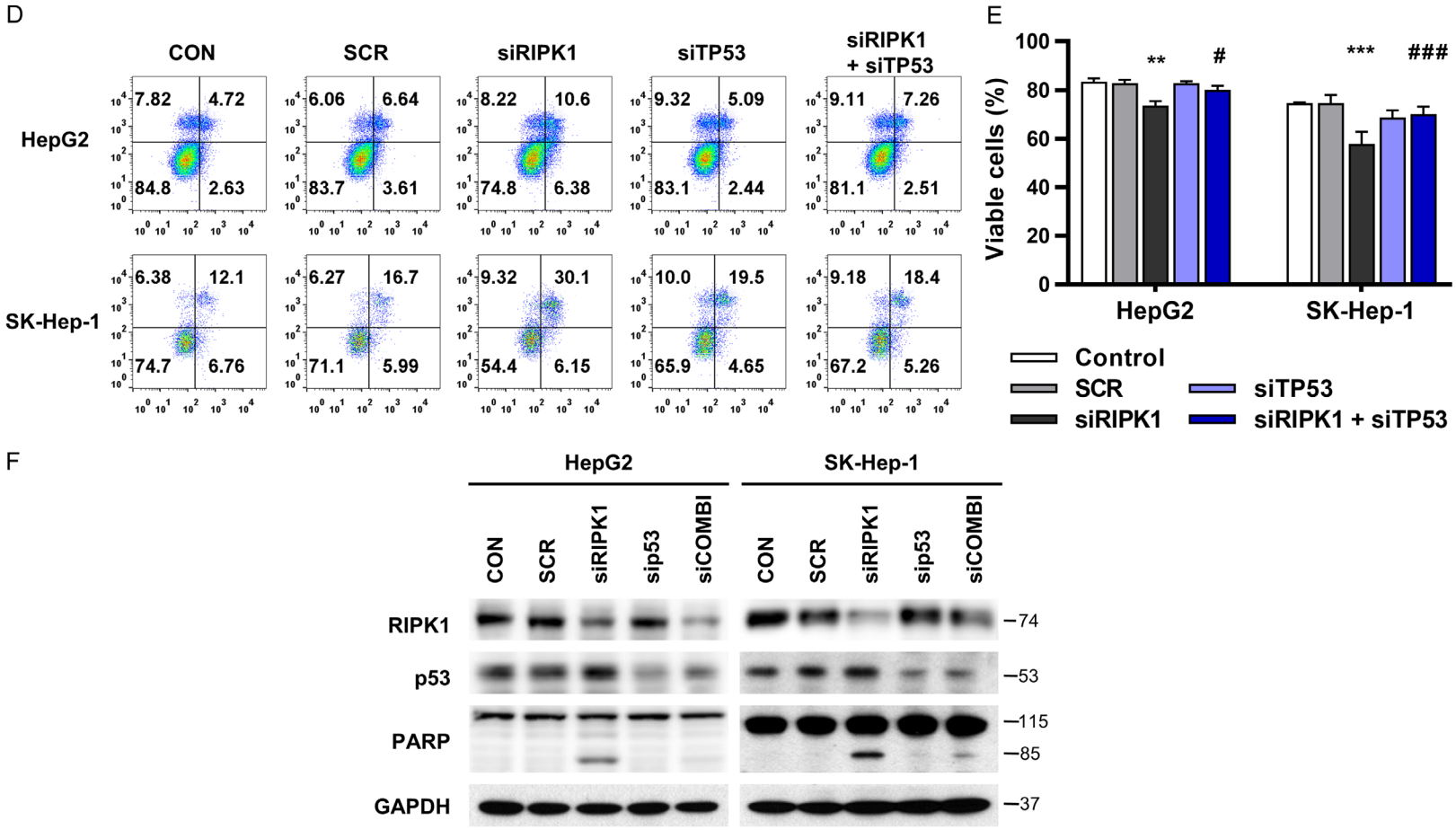

Figure 3. RIPK1 suppression induces apoptosis in a p53-dependent manner. (A) Western blot analysis of the indicated cell lines transfected with siRNAs for 72 h. siRIPK1-induced p53 induction was only observed in cells with wild-type p53. (B) Cell-cycle analysis of cells treated as in (A). (C) Graphs represent cell cycle analysis results obtained from three independent experiments. (D) Annexin V-APC and PI staining of HepG2 and SK-Hep-1 cells transfected with siRNAs for 72 h, as analyzed using FlowJo software. (E) Surviving cell population in the Annexin V/PI staining. Data represent the percentage ± SD; $^{**}P < 0.01$, $^{***}P < 0.001$ vs. control, $^{\#}P < 0.05$, $^{\#\#\#}P < 0.001$ vs. siRIPK1. (F) Western blot analysis of cells treated as in (D).

cell population. However, no significant cell cycle perturbations were observed in mt-p53 cells (**Figure 3B**, **3C**).

To clarify the role of p53 in siRIPK1-induced apoptosis, we simultaneously knocked down p53 and RIPK1 in cells harboring wt-p53. Transfection with siRNAs targeting p53 did not alter the viability of HepG2 cells but slightly increased the degree of apoptosis in SK-Hep-1 cells. Conversely, the simultaneous inhibition of RIPK1 and p53 slightly reduced siRIPK1-induced apoptosis (**Figure 3D**, **3E**). Although RIPK1 knockdown increased p53 expression, suppressing p53 did not alter RIPK1 expression. Interestingly, the simultaneous knockdown of RIPK1 and p53 attenuated the increase in PARP cleavage caused by RIPK1 suppression (**Figure 3F**). Thus, these results suggest that p53 may act downstream of RIPK1 and play an important role in siRIPK1-mediated apoptosis.

RIPK1 suppression induces DNA damage via the ROS-STAT3-ATR axis

p53 is a tumor suppressor that plays a central role in the cellular response to DNA damage caused by diverse stressors via the transcriptional activation of genes involved in cell cycle arrest, DNA repair, survival, senescence, and apoptosis [13, 14]. In HCC cells, oxidative stress and hepatitis virus-driven oncogenic replicative stress are common stimuli that elicit cellular responses. Treating HepG2 and SK-Hep-1 cells with siRIPK1 significantly increased ROS generation compared to cells with mt-p53 (**Figure 4A**, **4B**). In addition, RIPK1 knockdown in wt-p53 cells significantly decreased the expression of GPX-1, an antioxidant enzyme involved in ROS generation, but did not affect manganese superoxide dismutase (SOD2) or catalase levels (**Figure 4C**).

As RIPK1 suppression increased ROS levels, we next examined whether RIPK1 is associated with the DNA damage response by measuring the levels of γH2AX, a sensitive DNA damage marker [15]. Consistent with the above results, siRIPK1 remarkably increased γH2AX expression in wt-p53-expressing cell lines, but it did not alter γH2AX expression in mt-p53-expressing cells (**Figure 4D**). In addition, RIPK1 knockdown significantly decreased the total and phosphorylated forms of the DNA damage-sensing protein, ATR, and decreased the expression of topoisomerase II-binding protein 1, which plays a key role in ATR pathway activation, in cell lines expressing wt-p53. The observed decrease in ATR activation appears to conflict with p53 induction by siRIPK1; therefore, we investigated the involvement of STAT3, which regulates ATR to control DNA damage and is highly associated with the development of chronic liver disease and HCC [16-18]. As expected, RIPK1 knockdown reduced STAT3 activation in wt-p53 cells but no alteration was noted in mt-p53 cells, indicating that STAT3 inhibition contributes toward siRIPK1-mediated ATR inactivation and is closely associated with p53 status. In addition, siRNA-mediated p53 inhibition reversed the expression levels of γH2AX, pATR, and pSTAT3 induced by RIPK1 suppression (**Figure 4E**). Together, these results suggest that RIPK1 knockdown induces ROS-mediated DNA damage and apoptosis by suppressing STAT3-ATR activation in liver cancer cells harboring the wt-p53 protein.

STAT3 or ATR inhibition sensitizes cells with mt-p53 to siRIPK1-induced apoptosis

Notable, as mt-p53 HCC cells exhibit resistance to siRIPK1-induced cell death, we investigated whether the regeneration of p53 function by APR-246 (PRIMA-1^{MET}) restores sensitivity to siRIPK1 treatment [19]. As presented in **Figure 5A** and **5B**, compared to each treatment alone, treatment with APR-246 with siRIPK1 increased cleaved caspase-3 and PARP levels and significantly reduced cell viability in mt-p53 SNU449 cells. However, no additive effect was observed in Huh-7 cells.

Furthermore, given that RIPK1 suppression did not reduce STAT3 or ATR expression in mt-p53 HCC cells, we investigated whether a combination treatment could increase cell death. Huh-7 and SNU449 cells were treated with siRIPK1 alongside STAT3 or ATR knockdown. Because STAT3 or ATR suppression alone induced marked apoptosis in Huh-7 cells to a degree similar to that of siRIPK-induced apoptosis, no further decrease in cell viability by the combination treatment was observed. However, combined knockdown of RIPK and STAT3 in SNU449 cells increased cleaved caspase-3 and PARP levels more than siRIPK1 or siSTAT3 alone. In addition, RIPK1 and ATR

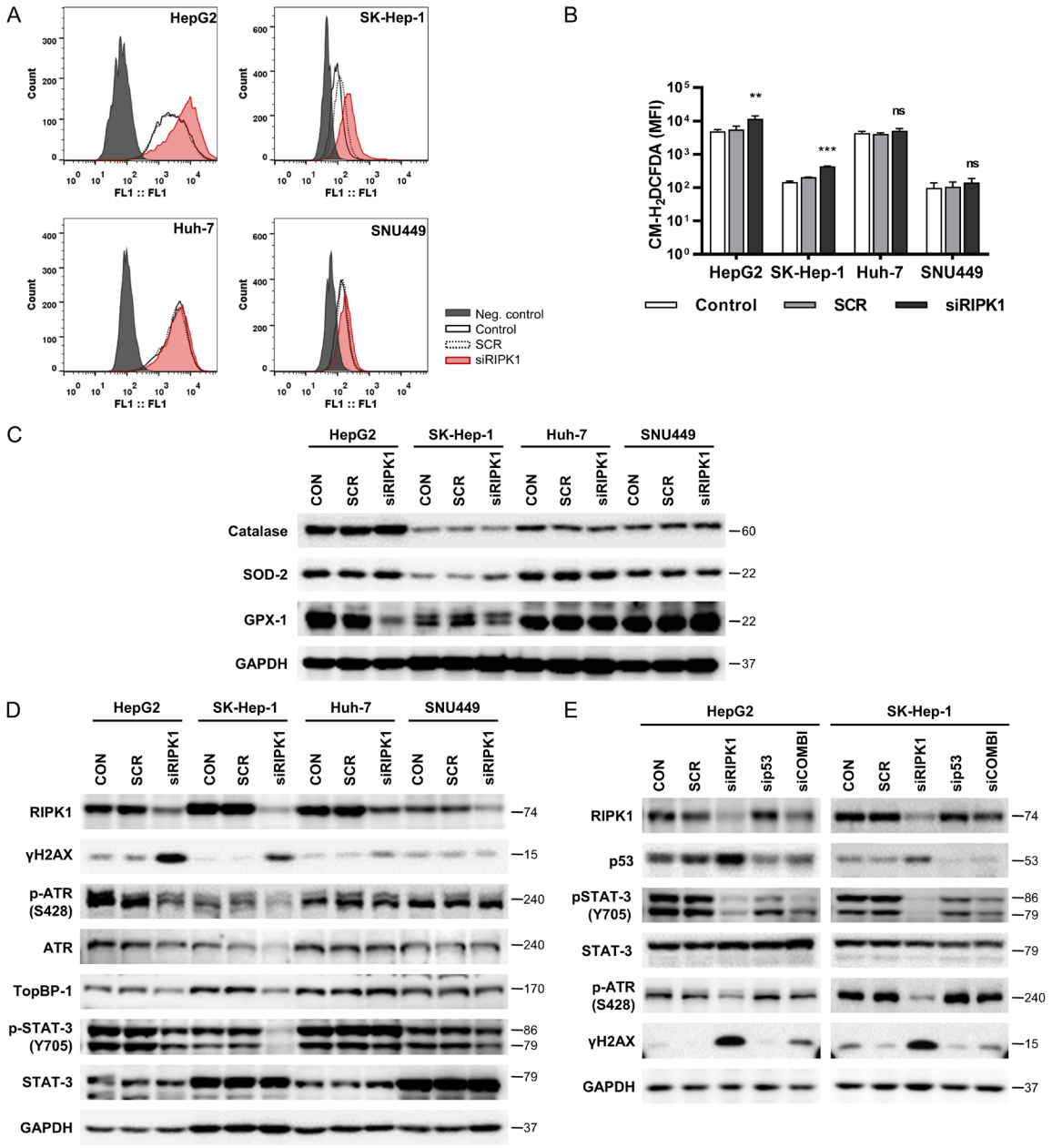

Figure 4. RIPK1 suppression induces DNA damage via the ROS/STAT3/ATR axis. (A) Total cellular ROS production of cells transfected with siRNAs for 72 h and stained with CM-H_2DCFDA, as measured using flow cytometry. (B) Data represent the mean ± SD of three independent experiments. $^{**}P < 0.01$, $^{***}P < 0.001$ vs. control. (C) Western blot analysis of antioxidant enzymes in the indicated cell lines transfected with siRNAs for 72 h. (D) Western blot analysis of DNA damage and STAT3 in cells treated as in (C). (E) Western blot analysis of the role of p53 on siRIPK1-induced STAT3-ATR suppression in HepG2 and SK-Hep-1 cells transfected with siRNAs for 72 h.

knockdown further increased caspase-3 and PARP cleavage compared to siRIPK1 or siATR alone, indicating that inhibition of STAT3 or ATR may attenuate resistance to siRIPK treatment in mt-p53 cells (**Figure 5C-E**). These results suggest that STAT3 and ATR may be promising targets for sensitizing mt-p53 HCC cells that are resistant to siRIPK1-induced apoptosis.

Clinical significance of RIPK1 expression in patients with liver hepatocellular carcinoma (LIHC)

Finally, we analyzed the clinical significance of RIPK1 and its potential as an anticancer therapeutic target using public expression profiles with GEPIA2. RIPK1 expression was significant-

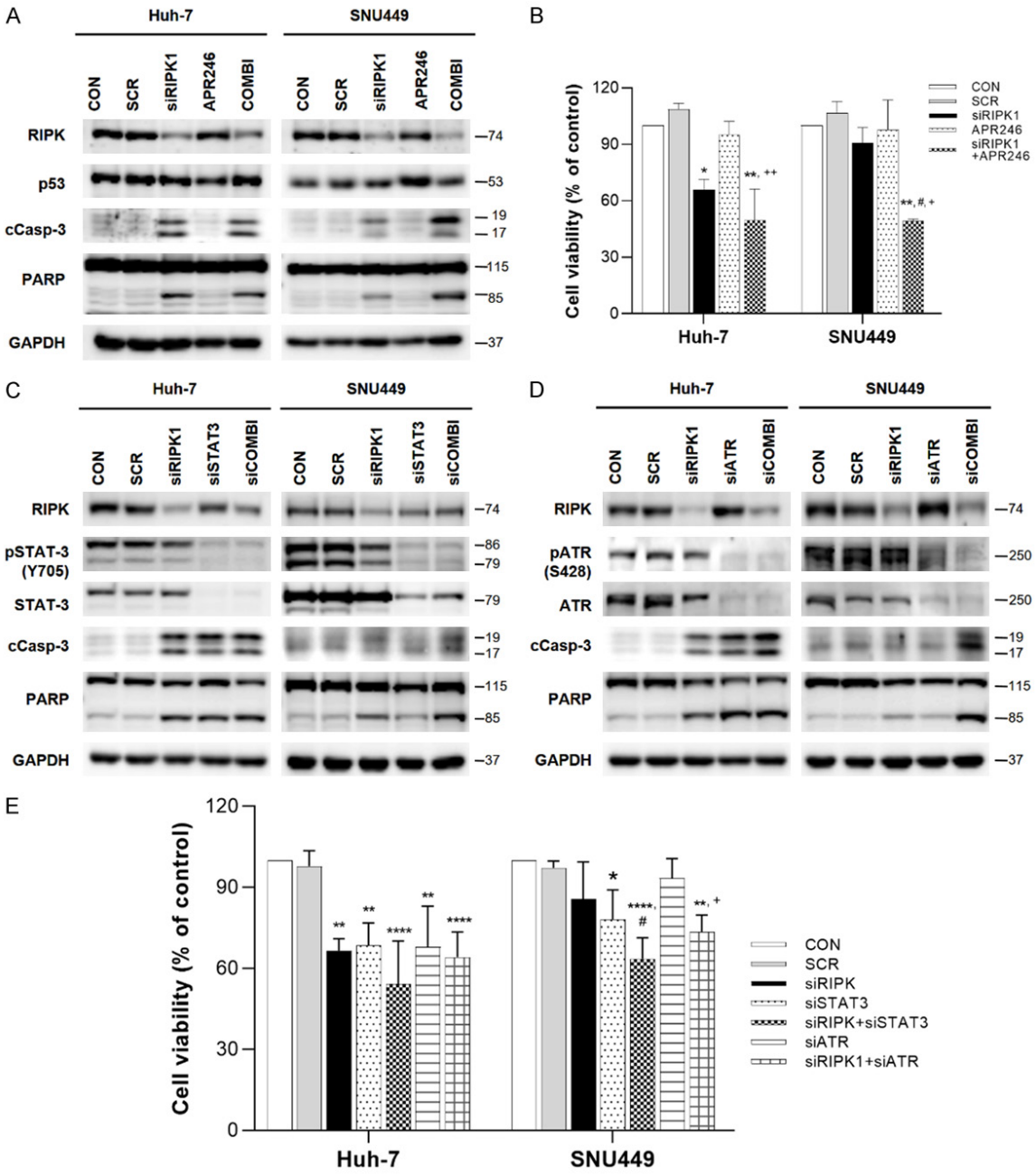

Figure 5. STAT3 or ATR suppression in mutant p53 cells restores sensitivity to siRIPK1-induced apoptosis. (A) Reactivation of the transcriptional activity of p53 mutants by APR-246 increased cleaved caspase-3 and PARP, as determined by western blot. (B) MTT assay was performed to investigate the cell viability of APR-246 treatment in mt-p53 HCC cells. $^{*}P < 0.05$, $^{**}P < 0.01$ vs. control, $^{\#}P < 0.05$ vs. siRIPK1, $^{+}P < 0.05$, $^{++}P < 0.01$ vs. APR-246. (C, D) Western blot analysis of Huh-7 and SNU449 cells transfected with the indicated siRNA for STAT3 (C) or ATR (D). (E) Viability of Huh-7 and SNU449 cells transfected with the indicated siRNA for STAT3 or ATR by MTT assay. Data represent the mean ± SD of at least three independent experiments. Significant differences were determined using ANOVA with Tukey's post-hoc test; $^{*}P < 0.05$, $^{**}P < 0.01$, $^{****}P < 0.0001$ vs. control, $^{\#}P < 0.05$ vs. siRIPK1, $^{+}P < 0.05$ vs. siATR.

ly higher in glioblastoma, cholangiocarcinoma, pancreatic adenocarcinoma, and thymoma than in adjacent normal tissues, but was slightly higher in LIHC (9.77 transcripts per million (TPM) in tumor vs. 8.71 TPM in matched normal tissue). In addition, RIPK1 expression was significantly higher in stage 1 to stage 3 LIHC than in adjacent normal tissues (data not shown). Subsequent analysis of the association between RIPK1 expression and patient

survival showed that RIPK1 expression was associated with a better OS in patients with kidney renal clear cell carcinoma but with a worse OS and disease-free survival (DFS) in patients with brain lower grade glioma. Although LIHC patients with high RIPK1 expression showed poor survival, this difference was not statistically significant (**Figure 6A**). According to Kaplan-Meier analysis, the hazard ratio (HR) of RIPK1 was increased significantly by the presence of hepatitis virus but not by alcohol consumption (**Figure 6B**). Since several studies have demonstrated that STAT3 plays a key role in viral replication [18, 20], we analyzed the correlation between RIPK1 and STAT3. In patients with LIHC, RIPK1 and STAT3 expression displayed a moderate positive correlation; however, no correlation was observed between RIPK1 and ATR or RIPK1 and p53. Genotype-tissue expression (GTEx) revealed a moderate positive correlation between RIPK1 and ATR or RIPK1 and p53 in healthy tissues. Taken together, these results indicate that a loss of correlation between RIPK1 and ATR or p53 expression may be associated with the carcinogenesis of liver cancer.

Discussion

RIPK1 tightly regulates cell survival, apoptosis, and necroptosis through NF-κB, caspase-8, and RIPK3, respectively [3, 4, 21]. Under normal physiological conditions *in vivo*, RIPK1 promotes cell survival via the canonical NF-κB pathway in the presence of TNF-α [9, 22, 23]; however, if cell death signaling is stronger than the survival signals, RIPK1 can induce apoptosis through the RIPK1-Fas-associated death domain protein scaffold to activate caspase-8. When caspase-8 is blocked by viral proteins or z-VAD-fmk under apoptotic conditions, RIPK1 promotes necroptosis by binding RIPK3 and MLKL. Although these signaling pathways are comparatively well defined, the cellular effects of RIPK1 suppression itself and the fate of RIPK1 deficient cells remain largely unknown. In addition, the majority of studies have examined RIPK1 under artificial conditions, such as combined treatment with TNF-α and CHX [24, 25] or under conditions of FasL activation, oxidative stress, radiation, and DNA damage-inducing anticancer agents. Few have studied the effects and mechanism of RIPK1 under normal conditions.

Because the liver is often exposed to chronic injury and inflammatory conditions that may be associated with RIPK1 [4, 21], we decided to examine the effects of RIPK1 knockdown in HCC cells. Silencing RIPK1 with siRNAs reduced the viability of HCC cells and significantly increased the degree of apoptosis in wt-p53 cells but not in mt-p53 cells. Interestingly, we found that siRIPK1 reduced ATR expression in a p53-dependent manner. DNA damage induces either pATM or pATR, which phosphorylate H2AX to activate the p53 protein and thereby promote cell-cycle arrest and apoptosis [15, 26]. ATR is a DNA damage sensor kinase that plays an essential role regulating cell viability during replication stress, with ATR suppression sensitizing HeLa cells to DNA damage and inducing γH2AX expression [27-30]. However, siRIPK1 did not alter ATR or γH2AX activation in cells expressing mt-p53 or during p53 silencing, suggesting that p53 may function as an executioner of apoptosis rather than in the DNA damage repair response. Similar to our results indicating that siRIPK1-mediated apoptosis is dependent on p53, several studies have shown a correlation between RIPK1 and p53. RIPK1 suppression has been reported to induce p53 overexpression in glioblastoma and MEF cells by downregulating mdm2, which is associated with NF-κB inactivation [31]. In addition, RIPK1 suppression has been shown to inhibit the proliferation of A549 lung cancer cells in a p53-dependent manner by inducing mitochondrial oxidative phosphorylation defects, excessive glycolysis, and DNA damage [32]. Recently, it was reported that RIPK1 is essential for the survival of bone marrow mesenchymal stem cells and functions by maintaining mitochondrial homeostasis in a p53-dependent manner [33]. In contrast, it has been documented that diverse anticancer agents induce p53-independent cell death through RIPK1-JNK signaling pathway activation [34, 35] or p53-dependent cell death via the RIPK1/3-ROS-JNK-p53 axis [36]. Therefore, as RIPK1 and p53 are important factors that can regulate both cell survival and death, the eventual fate of cells might vary depending on the circumstances under which they are expressed.

Another aspect of RIPK1 expression that remains unclear is the mechanism via which RIPK1 suppression induces DNA damage. Although ROS are one of the most important

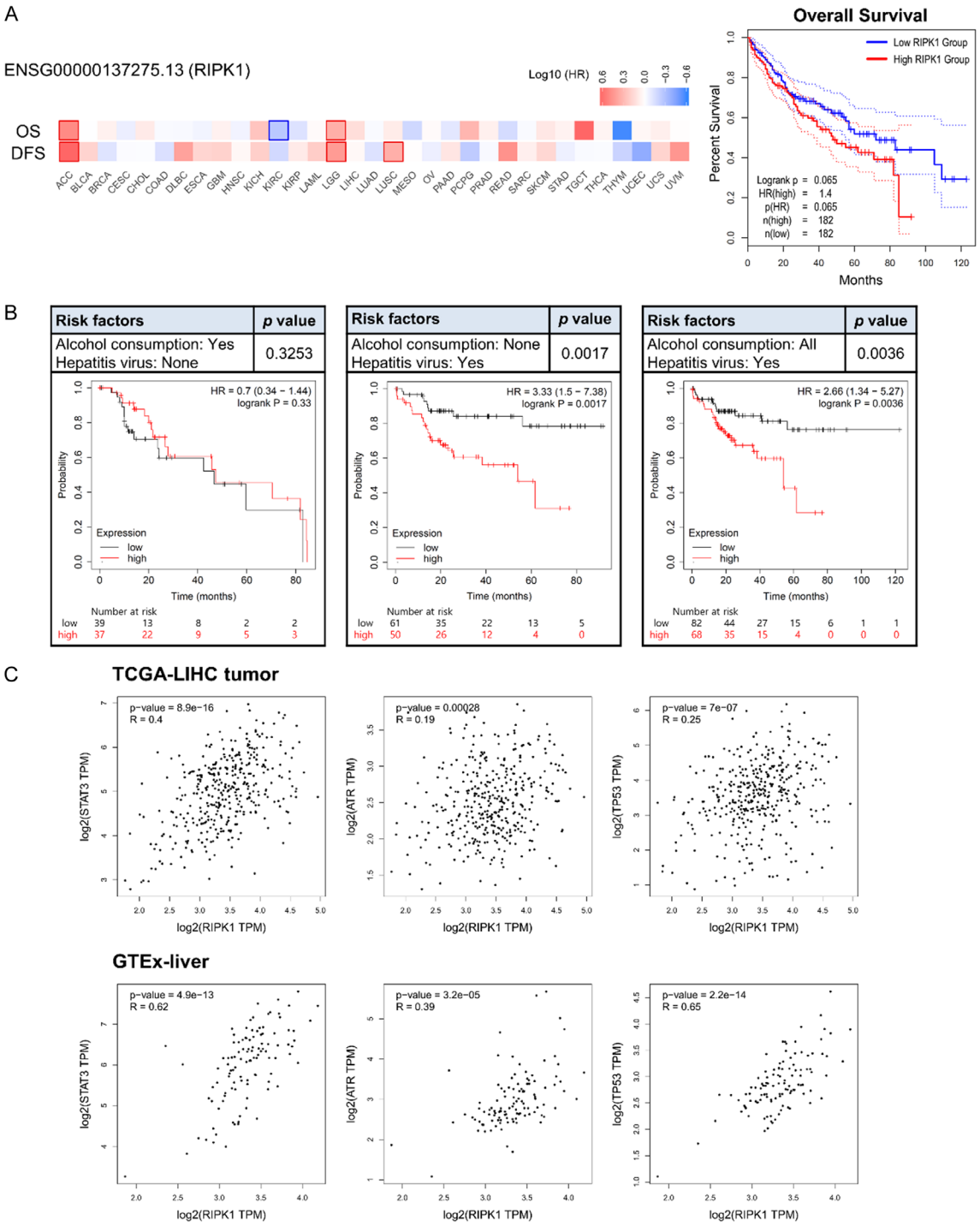

Figure 6. Clinical significance of RIPK1. A. OS and DFS of RIPK1. B. Kaplan-Meier survival analysis of RIPK1 in LIHC in the presence of different risk factors. C. Correlation between RIPK1 and STAT3, ATR, or p53 in TCGA-LIHC tumors (upper panel) and in GTEx-livers (lower panel) analyzed using Pearson correlation analysis.

inducers of DNA damage and genomic instability [37], they are produced at high levels by mitochondria in cancer cells and play an essential role in cancer cell survival by maintaining the activation of STAT3 and other oncogenic pathways [38]. Cancer cells may also utilize endogenous ROS-scavenging antioxidant enzymes to attenuate cytotoxicity induced by

chemotherapeutic drugs. For instance, Wang et al. reported that RIPK1 increases chemoresistance by reducing ROS generation via miRNA-146a-mediated catalase suppression [39]. Here, we demonstrated that siRIPK1 significantly increased ROS levels to varying degrees in different liver cancer cell types. RIPK1 knockdown also decreased the levels of GPX-1, which is the major GPX in the mammalian liver and contributes toward the prevention of mitochondrial oxidative stress [40]. Consequently, RIPK1 suppression may induce the accumulation of cellular stressors, such as ROS, leading to extensive DNA damage; however, further studies are required to elucidate the exact mechanism of GPX-1 downregulation.

Interestingly, siRIPK1-induced ROS generation and DNA damage were not observed in mt-p53 cells. Therefore, we investigated whether STAT3, a negative regulator of p53 and an upstream molecule of ATR, was involved in the resistance to siRIPK1-induced apoptosis. Abnormal STAT3 activation is closely related to the occurrence, proliferation, drug resistance, and stemness of various tumors, including HCC, and plays an important role in the regulation of complex networks formed in the tumor microenvironment [41-43]. Importantly, siRIPK1-mediated STAT3 inhibition was not observed in the absence of p53 but was evident in wt-p53 cells upon p53 induction. Several studies have shown that STAT3 can inhibit p53 by binding to the repressor of the p53 promoter, while p53 can suppress STAT3 phosphorylation and DNA-binding activity, suggesting that the two proteins have opposite and reciprocal functions [38, 42, 44]. The mt-p53 HCC cells resist siRIPK1-induced cell death by keeping STAT3 expression unchanged, whereas the regeneration of p53 function by APR-246 or depletion of STAT3 in mt-p53 cells reduces this resistance. Therefore, these results suggest that p53 and STAT3 may be important regulators in determining the sensitivity of HCC cells to siRIPK1-induced cell death. Several studies have demonstrated the connection between RIPK1 and STAT3. RIPK1 promotes the radiation-induced invasion of non-small cell lung cancer cells via the Src/STAT3-EMT pathway [45]. In addition, IL6-mediated STAT3-DNMT activation blocks TNFα-RIPK1-induced necroptosis in myeloid-derived suppressor cells [46]. Recent data have also shown that in addition to the metabolic role of mitochondrial STAT3, the phosphorylation of STAT3 at Ser727 can result in its translocation to the mitochondria to induce ROS-mediated cell death [47, 48]. Like RIPK1 and p53 mentioned previously herein, STAT3 is also implicated in cell fate decisions as an anti-apoptotic and a pro-death factor [49]. Therefore, the involvement of STAT3 in the RIPK1-NF-κB pathway or RIPK1-mediated necroptosis has been somewhat reported, but it remains controversial, and the exact signaling cascades involved need to be elucidated. Although we investigated the effect of RIPK1 silencing in only four cell lines, the combination of STAT3 or ATR and RIPK1 inhibition is a promising alternative approach for cancer cells harboring mt-p53. However, the results were cell-dependent and the inhibition of each target alone occasionally induced sufficient cell death. Therefore, further studies should be conducted to establish optimal treatment conditions validating the additive or synergistic effects of these combinations.

Consequently, we propose a hypothesis for the role of p53 and STAT3 in RIPK1 knockdown in liver cancer cells (**Figure 7**). In the absence of exogenous stimulation, RIPK1 promoted liver cancer cell growth through the STAT3/ATR survival pathway without activating p53. However, RIPK1 silencing in wt-p53 liver cancer cells inhibited the STAT3/ATR-mediated DNA damage repair response and increased p53 expression, resulting in p53-mediated proliferation inhibition. In HCC with mutant inactive p53, siRIPK1 decreased STAT3-mediated survival pathways, which were restored by the loss of the STAT3-repressive ability of mt-p53. Nonetheless, the decreased viability of Huh-7 and SNU449 cells with mt-p53 caused by RIPK1 suppression may partially be due to the involvement of other STATs, particularly STAT5, or the inhibition of NF-κB survival pathways, although further studies are required to elucidate the underlying molecular mechanism.

RIPK1 is thought to promote the growth of cancer cells via the NF-κB survival pathway; however, we found that RIPK1 was not highly expressed in all tested cell lines. In addition, bioinformatic analyses indicated that RIPK1 had low tissue- or cell-type specificity. High RIPK1 expression was associated with poor survival in patients with LIHC, but without statistical significance. Interestingly, the HR for

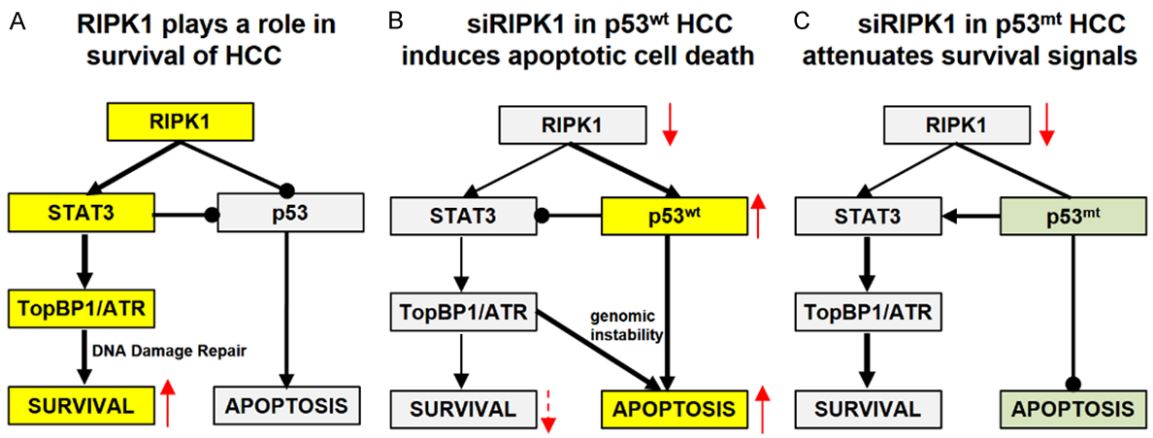

Figure 7. Proposed model of the roles of p53 and STAT3 following RIPK1 knockdown in liver cancer cells. A. In the absence of exogenous stimulation, RIPK1 promotes the growth of liver cancer cells through the STAT3/ATR survival pathway or NF-κB signaling (not shown). Since p53 is maintained at low levels by ubiquitination-mediated proteasomal degradation, it is not activated under unstressed conditions [56]. B. During RIPK1 silencing, p53 expression is increased and the STAT3/ATR-mediated DNA damage repair response is inhibited, resulting in the apoptosis of liver cancer cells with wild type p53. C. RIPK1 knockdown in liver cancer cells with mutant inactivated p53 decreases STAT3-mediated survival pathways but is moderately restored by the loss of the STAT3-repressive ability of mutant p53. Arrows indicate activating interactions and lines terminating in a circle indicate repressive interactions.

RIPK1 increased significantly in the presence of hepatitis virus, which is one of the main risk factors for HCC, alongside aflatoxin-contaminated foodstuffs, heavy alcohol intake, and type 2 diabetes [50]. Recent studies have attempted to develop new RIPK1 targeted drugs to overcome necrosis-associated pathological conditions, including ischemia/reperfusion injury and myocardial infarction [7, 51, 52]. Although necroptosis is likely to switch to apoptosis, these approaches could be effective under severe conditions [53-55]. In the current study, we first showed how differences in intrinsic RIPK1 expression in HCC affect cell survival and the mechanisms involved. The relationship between RIPK1 and p53 or between RIPK1 and STAT3 has been reported, but the intrinsic connections among RIPK1, p53, and STAT3 have not been elucidated. Because all three factors are critically involved in cell fate and are intricately linked to each other, our results could help to understand chemotherapy non-response and resistance. Taken together with these previous studies, our findings suggest that RIPK1 could be a promising target for treating cancer alone or in combination.

Conclusion

Treatment outcomes for liver cancer, a type of heterogeneous malignant disease caused by multiple etiology, remain unsatisfactory. The findings of this study demonstrate that RIPK1 suppression in liver cancer cells induces apoptosis by inhibiting the STAT3/ATR signaling pathways in a p53-dependent manner. Furthermore, our findings indicate that RIPK1 could be an attractive target for cancer treatment in combination with STAT3 or ATR inhibitors, particularly for patients with liver cancer carrying mt-p53 cells.

Acknowledgements

This study was supported by the National Research Foundation of Korea (NRF-2020R1A2C-1007138; NRF-2020M2D9A2094153) and the Korean Institute of Radiological and Medical Sciences (50531-2021) funded by the Korean government Ministry of Science and ICT.

Disclosure of conflicts of interest

None.

Address correspondence to: Jie-Young Song, Division of Radiation Biomedical Research, Korea Institute of Radiological & Medical Sciences, Seoul 01812, Republic of Korea. Tel: 82-2-970-1308; E-mail: immu@kirams.re.kr

References

[1] Kroemer G, Galluzzi L, Vandenabeele P, Abrams J, Alnemri ES, Baehrecke EH, Blagosklonny MV, El-Deiry WS, Golstein P, Green DR,

Hengartner M, Knight RA, Kumar S, Lipton SA, Malorni W, Nuñez G, Peter ME, Tschopp J, Yuan J, Piacentini M, Zhivotovsky B and Melino G; Nomenclature Committee on Cell Death 2009. Classification of cell death: recommendations of the Nomenclature Committee on Cell Death 2009. Cell Death Differ 2009; 16: 3-11.

[2] Brenner D, Blaser H and Mak TW. Regulation of tumour necrosis factor signalling: live or let die. Nat Rev Immunol 2015; 15: 362-374.

[3] Feoktistova M and Leverkus M. Programmed necrosis and necroptosis signalling. FEBS J 2015; 282: 19-31.

[4] Silke J, Rickard JA and Gerlic M. The diverse role of RIP kinases in necroptosis and inflammation. Nat Immunol 2015; 16: 689-697.

[5] Vanden Berghe T, Linkermann A, Jouan-Lanhouet S, Walczak H and Vandenabeele P. Regulated necrosis: the expanding network of non-apoptotic cell death pathways. Nat Rev Mol Cell Biol 2014; 15: 135-147.

[6] Blander JM. A long-awaited merger of the pathways mediating host defence and programmed cell death. Nat Rev Immunol 2014; 14: 601-618.

[7] Jouan-Lanhouet S, Riquet F, Duprez L, Vanden Berghe T, Takahashi N and Vandenabeele P. Necroptosis, in vivo detection in experimental disease models. Semin Cell Dev Biol 2014; 35: 2-13.

[8] Mocarski ES, Upton JW and Kaiser WJ. Viral infection and the evolution of caspase 8-regulated apoptotic and necrotic death pathways. Nat Rev Immunol 2011; 12: 79-88.

[9] O'Donnell MA and Ting AT. NFkappaB and ubiquitination: partners in disarming RIPK1-mediated cell death. Immunol Res 2012; 54: 214-226.

[10] Robinson MW, Harmon C and O'Farrelly C. Liver immunology and its role in inflammation and homeostasis. Cell Mol Immunol 2016; 13: 267-276.

[11] Weber A, Boege Y, Reisinger F and Heikenwalder M. Chronic liver inflammation and hepatocellular carcinoma: persistence matters. Swiss Med Wkly 2011; 141: w13197.

[12] Szabo G and Petrasek J. Inflammasome activation and function in liver disease. Nat Rev Gastroenterol Hepatol 2015; 12: 387-400.

[13] Joerger AC and Fersht AR. The p53 pathway: origins, inactivation in cancer, and emerging therapeutic approaches. Annu Rev Biochem 2016; 85: 375-404.

[14] Oren M. Decision making by p53: life, death and cancer. Cell Death Differ 2003; 10: 431-442.

[15] Mah LJ, El-Osta A and Karagiannis TC. gammaH2AX: a sensitive molecular marker of DNA damage and repair. Leukemia 2010; 24: 679-686.

[16] Rosmorduc O and Desbois-Mouthon C. Targeting STAT3 in hepatocellular carcinoma: sorafenib again. J Hepatol 2011; 55: 957-959.

[17] Liao XH, Zheng L, He HP, Zheng DL, Wei ZQ, Wang N, Dong J, Ma WJ and Zhang TC. STAT3 regulated ATR via microRNA-383 to control DNA damage to affect apoptosis in A431 cells. Cell Signal 2015; 27: 2285-2295.

[18] Lian X, Bao C, Li X, Zhang X, Chen H, Jung YS and Qian Y. Marek's disease virus disables the ATR-Chk1 pathway by activating STAT3. J Virol 2019; 93: e02290-18.

[19] Wiman KG. Pharmacological reactivation of mutant p53: from protein structure to the cancer patient. Oncogene 2010; 29: 4245-4252.

[20] Koganti S, Hui-Yuen J, McAllister S, Gardner B, Grasser F, Palendira U, Tangye SG, Freeman AF and Bhaduri-McIntosh S. STAT3 interrupts ATR-Chk1 signaling to allow oncovirus-mediated cell proliferation. Proc Natl Acad Sci U S A 2014; 111: 4946-4951.

[21] Ofengeim D and Yuan J. Regulation of RIP1 kinase signalling at the crossroads of inflammation and cell death. Nat Rev Mol Cell Biol 2013; 14: 727-736.

[22] Gentle IE, Wong WW, Evans JM, Bankovacki A, Cook WD, Khan NR, Nachbur U, Rickard J, Anderton H, Moulin M, Lluis JM, Moujalled DM, Silke J and Vaux DL. In TNF-stimulated cells, RIPK1 promotes cell survival by stabilizing TRAF2 and cIAP1, which limits induction of non-canonical NF-kappaB and activation of caspase-8. J Biol Chem 2011; 286: 13282-13291.

[23] Wu YT, Tan HL, Huang Q, Sun XJ, Zhu X and Shen HM. zVAD-induced necroptosis in L929 cells depends on autocrine production of TNFalpha mediated by the PKC-MAPKs-AP-1 pathway. Cell Death Differ 2011; 18: 26-37.

[24] Bhattacharya S, Ray RM, Viar MJ and Johnson LR. Polyamines are required for activation of c-Jun NH2-terminal kinase and apoptosis in response to TNF-alpha in IEC-6 cells. Am J Physiol Gastrointest Liver Physiol 2003; 285: G980-991.

[25] Jin S, Ray RM and Johnson LR. TNF-alpha/cycloheximide-induced apoptosis in intestinal epithelial cells requires Rac1-regulated reactive oxygen species. Am J Physiol Gastrointest Liver Physiol 2008; 294: G928-937.

[26] Awasthi P, Foiani M and Kumar A. ATM and ATR signaling at a glance. J Cell Sci 2015; 128: 4255-4262.

[27] Brown EJ and Baltimore D. ATR disruption leads to chromosomal fragmentation and early embryonic lethality. Genes Dev 2000; 14: 397-402.

[28] Southgate HED, Chen L, Tweddle DA and Curtin NJ. ATR inhibition potentiates PARP inhibitor cytotoxicity in high risk neuroblastoma cell

lines by ultiple mechanisms. Cancers (Basel) 2020; 12: 1095.
[29] Ha K, Fiskus W, Rao R, Balusu R, Venkannagari S, Nalabothula NR and Bhalla KN. Hsp90 inhibitor-mediated disruption of chaperone association of ATR with hsp90 sensitizes cancer cells to DNA damage. Mol Cancer Ther 2011; 10: 1194-1206.
[30] de Klein A, Muijtjens M, van Os R, Verhoeven Y, Smit B, Carr AM, Lehmann AR and Hoeijmakers JH. Targeted disruption of the cell-cycle checkpoint gene ATR leads to early embryonic lethality in mice. Curr Biol 2000; 10: 479-482.
[31] Park S, Hatanpaa KJ, Xie Y, Mickey BE, Madden CJ, Raisanen JM, Ramnarain DB, Xiao G, Saha D, Boothman DA, Zhao D, Bachoo RM, Pieper RO and Habib AA. The receptor interacting protein 1 inhibits p53 induction through NF-kappaB activation and confers a worse prognosis in glioblastoma. Cancer Res 2009; 69: 2809-2816.
[32] Chen W, Wang Q, Bai L, Chen W, Wang X, Tellez CS, Leng S, Padilla MT, Nyunoya T, Belinsky SA and Lin Y. RIP1 maintains DNA integrity and cell proliferation by regulating PGC-1alpha-mediated mitochondrial oxidative phosphorylation and glycolysis. Cell Death Differ 2014; 21: 1061-1070.
[33] Tian Q, Cao C, Qiu W, Wu H, Zhou L, Dai Z, Li Z and Chen S. RIPK1 coordinates bone marrow mesenchymal stem cell survival by maintaining mitochondrial homeostasis via p53. Stem Cells Int 2021; 2021: 5540149.
[34] Hur GM, Kim YS, Won M, Choksi S and Liu ZG. The death domain kinase RIP has an important role in DNA damage-induced, p53-independent cell death. J Biol Chem 2006; 281: 25011-25017.
[35] Biton S and Ashkenazi A. NEMO and RIP1 control cell fate in response to extensive DNA damage via TNF-alpha feedforward signaling. Cell 2011; 145: 92-103.
[36] Zhang L, Wang H, Ding K and Xu J. FTY720 induces autophagy-related apoptosis and necroptosis in human glioblastoma cells. Toxicol Lett 2015; 236: 43-59.
[37] Turgeon MO, Perry NJS and Poulogiannis G. DNA damage, repair, and cancer metabolism. Front Oncol 2018; 8: 15.
[38] Granato M, Gilardini Montani MS, Santarelli R, D'Orazi G, Faggioni A and Cirone M. Apigenin, by activating p53 and inhibiting STAT3, modulates the balance between pro-apoptotic and pro-survival pathways to induce PEL cell death. J Exp Clin Cancer Res 2017; 36: 167.
[39] Wang Q, Chen W, Bai L, Chen W, Padilla MT, Lin AS, Shi S, Wang X and Lin Y. Receptor-interacting protein 1 increases chemoresistance by maintaining inhibitor of apoptosis protein levels and reducing reactive oxygen species through a microRNA-146a-mediated catalase pathway. J Biol Chem 2014; 289: 5654-5663.
[40] Brigelius-Flohe R and Maiorino M. Glutathione peroxidases. Biochim Biophys Acta 2013; 1830: 3289-3303.
[41] Yu H, Lee H, Herrmann A, Buettner R and Jove R. Revisiting STAT3 signalling in cancer: new and unexpected biological functions. Nat Rev Cancer 2014; 14: 736-746.
[42] Wormann SM, Song L, Ai J, Diakopoulos KN, Kurkowski MU, Gorgulu K, Ruess D, Campbell A, Doglioni C, Jodrell D, Neesse A, Demir IE, Karpathaki AP, Barenboim M, Hagemann T, Rose-John S, Sansom O, Schmid RM, Protti MP, Lesina M and Algul H. Loss of P53 function activates JAK2-STAT3 signaling to promote pancreatic tumor growth, stroma modification, and gemcitabine resistance in mice and is associated with patient survival. Gastroenterology 2016; 151: 180-193, e112.
[43] Jones LM, Broz ML, Ranger JJ, Ozcelik J, Ahn R, Zuo D, Ursini-Siegel J, Hallett MT, Krummel M and Muller WJ. STAT3 establishes an immunosuppressive microenvironment during the early stages of breast carcinogenesis to promote tumor growth and metastasis. Cancer Res 2016; 76: 1416-1428.
[44] Niu G, Wright KL, Ma Y, Wright GM, Huang M, Irby R, Briggs J, Karras J, Cress WD, Pardoll D, Jove R, Chen J and Yu H. Role of Stat3 in regulating p53 expression and function. Mol Cell Biol 2005; 25: 7432-7440.
[45] Kang AR, Cho JH, Lee NG, Song JY, Hwang SG, Lee DH, Um HD and Park JK. RIP1 is a novel component of gamma-ionizing radiation-induced invasion of non-small cell lung cancer cells. Int J Mol Sci 2020; 21: 4584.
[46] Smith AD, Lu C, Payne D, Paschall AV, Klement JD, Redd PS, Ibrahim ML, Yang D, Han Q, Liu Z, Shi H, Hartney TJ, Nayak-Kapoor A and Liu K. Autocrine IL6-mediated activation of the STAT3-DNMT axis silences the TNFalpha-RIP1 necroptosis pathway to sustain survival and accumulation of myeloid-derived suppressor cells. Cancer Res 2020; 80: 3145-3156.
[47] Kim H, Zamel R, Bai XH, Lu C, Keshavjee S, Keshavjee S and Liu M. Ischemia-reperfusion induces death receptor-independent necroptosis via calpain-STAT3 activation in a lung transplant setting. Am J Physiol Lung Cell Mol Physiol 2018; 315: L595-L608.
[48] Sharapova TN, Romanova EA, Sashchenko LP and Yashin DV. FasL on the surface of Tag7 (PGRP-S)-activated lymphocytes induces necroptosis in HLA-negative tumor cells with the involvement of lysosomes and mitochondria. Biochimie 2018; 152: 174-180.

[49] Georgiadis V and Knight RA. Necroptosis: STAT3 kills? JAKSTAT 2012; 1: 200-202.
[50] Llovet JM, Zucman-Rossi J, Pikarsky E, Sangro B, Schwartz M, Sherman M and Gores G. Hepatocellular carcinoma. Nat Rev Dis Primers 2016; 2: 16018.
[51] Dannappel M, Vlantis K, Kumari S, Polykratis A, Kim C, Wachsmuth L, Eftychi C, Lin J, Corona T, Hermance N, Zelic M, Kirsch P, Basic M, Bleich A, Kelliher M and Pasparakis M. RIPK1 maintains epithelial homeostasis by inhibiting apoptosis and necroptosis. Nature 2014; 513: 90-94.
[52] Najjar M, Suebsuwong C, Ray SS, Thapa RJ, Maki JL, Nogusa S, Shah S, Saleh D, Gough PJ, Bertin J, Yuan J, Balachandran S, Cuny GD and Degterev A. Structure guided design of potent and selective ponatinib-based hybrid inhibitors for RIPK1. Cell Rep 2015; 10: 1850-1860.
[53] Orozco S, Yatim N, Werner MR, Tran H, Gunja SY, Tait SW, Albert ML, Green DR and Oberst A. RIPK1 both positively and negatively regulates RIPK3 oligomerization and necroptosis. Cell Death Differ 2014; 21: 1511-1521.
[54] Takahashi N, Vereecke L, Bertrand MJ, Duprez L, Berger SB, Divert T, Goncalves A, Sze M, Gilbert B, Kourula S, Goossens V, Lefebvre S, Gunther C, Becker C, Bertin J, Gough PJ, Declercq W, van Loo G and Vandenabeele P. RIPK1 ensures intestinal homeostasis by protecting the epithelium against apoptosis. Nature 2014; 513: 95-99.
[55] Vanlangenakker N, Bertrand MJ, Bogaert P, Vandenabeele P and Vanden Berghe T. TNF-induced necroptosis in L929 cells is tightly regulated by multiple TNFR1 complex I and II members. Cell Death Dis 2011; 2: e230.
[56] Liu B, Chen Y and St Clair DK. ROS and p53: a versatile partnership. Free Radic Biol Med 2008; 44: 1529-1535.